Monte Carlo diffusion simulations disambiguate the biophysical mechanisms of diffusion hinderance along tracts

Michiel Kleinnijenhuis[1], Jeroen Mollink[1], Paul Kinchesh[2], Wilfred W Lam[1], Vitaly L Galinsky[3], Lawrence R Frank[3], Sean C Smart[2], Saad Jbabdi[1], and Karla L Miller[1]

[1]FMRIB Centre, University of Oxford, Oxford, United Kingdom, [2]Department of Oncology, University of Oxford, Oxford, United Kingdom, [3]Center for Scientific Computation in Imaging, University of California San Diego, La Jolla, United States

PURPOSE – Diffusion imaging at long diffusion times can inform on microstructural features of tissue at scales spanning several hundreds of micrometers. At these scales the common approximation of axons as straight cylinders might not hold, even for tissues that are generally assumed to be coherently organized. The human corpus callosum is such a tract. It is often used as a reference structure for simple fibre configuration. Nevertheless, evidence from electron microscopy and histology suggests that corpus callosum fibres are far from coherent[1,2]. Fibres not only bend along the tract, but also twist and undulate, effects that could lead to specific signatures of hinderance "along" the tract. In this study, we investigated the diffusion time dependence of the apparent diffusion coefficient (ADC) along the direction of the fibres in the corpus callosum. Possible biophysical mechanisms of this dependence are explored by means of Monte Carlo simulations of various axon models.

Figure 1. *Simulated geometries. a) fanning and bending - each individual axon represents one of the bending geometries, the set forms the fanning geometry. b) undulating: helical geometry with molecules diffusing intracellularly.*

METHODS – **Postmortem MRI:** A 3x2 cm block of human brain tissue including the medial corpus callosum was cut from a 5 mm thick coronal slice at the level of the anterior commisure. The block was soaked in phosphate buffered saline for 72 hrs, transferred to a syringe filled with Fluorinert (3M) and scanned on a Varian 9.4T preclinical system using a 25 mm quadrature birdcage coil (Rapid Biomedical). Diffusion-weighted STEAM data were acquired with diffusion gradients (δ=2.22 ms) applied in 30 directions distributed over a hemisphere for 9 mixing times [24.3, 59.3, 89.3, 139.3, 189.3, 239.3, 289.3, 339.3, 389.3] ms with a fixed q-value (0.14 rad/µm; with removal of crusher gradients to avoid b-value contamination). For each mixing time, a non-diffusion weighted image was acquired. Imaging parameters: 10 slices with 400 µm isotropic voxels, TE=16ms, TR=2.4-4.1 s (minimized for each diffusion time). Spin-echo diffusion data were acquired with TR/TE=2.4s/29ms, 240 diffusion gradient directions (δ=6ms, Δ=16ms) with b=2500 and 5000 s*mm^{-2}. **Simulations:** Diffusion MR signal attenuation was calculated with the MR diffusion Monte Carlo simulator DifSim[3] that tracks the phase of each diffusing molecule throughout the simulated experiment. Simulations were performed in axons with various

degrees of bending, fanning and undulation. Axon models were created in Blender v2.70. Bending axons with a length of 50, 100 and 200 µm and a 0.5 µm radius were bent over [0, 45, …, 360] degrees, resulting in a spread of curvatures (Figure 1). Fanning configurations were created by combining the set of bending axons of a given length. Undulating axons were modeled as helixes with radius of 0.5 µm and height of 200 µm with [30, 50, 70, 90] turns over their length. Models were exported using the CellBlender v1.0.0 plugin for compatibility with diffusion-reaction simulator MCell v3.1[4] used by DifSim. In each model, 9600 molecules were released intracellularly (non-permeable membranes) at t=0 s from the plane bisecting the model at z=0. The simulation time was 402400 µs with a time step of 1 µs. The MR signal was calculated by DifSim for the same protocols as used in the postmortem MRI protocols (30 directions for 9 mixing times).
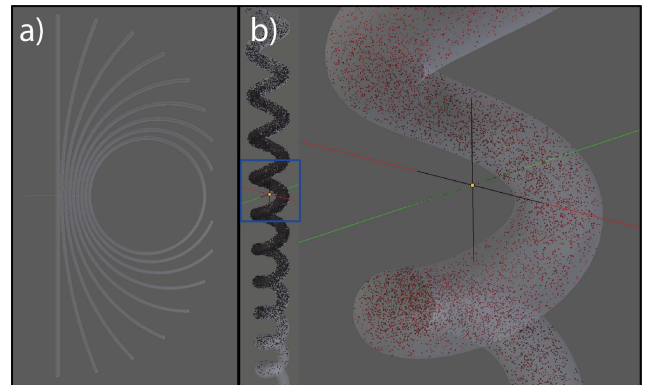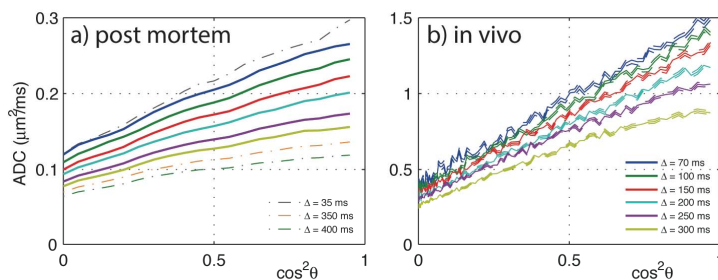

Figure 2. *ADC plotted against the cos^2 of the angle between the diffsion gradient and the primary diffusion direction. Similar patterns are seen for post mortem and in vivo data. Diffusion time dependence is seen perpendicular to the main fibre directions, but ADC also varies strongly with diffusion time along the fibres.*

RESULTS AND DISCUSSION – Figure 2 demonstrates the diffusion time dependence of the ADC for different orientations of the fibre (given as cos$^2\theta$, derived from a tensor fit to the SE DWI data). Post mortem data (Figure 2a) and in vivo data (Figure 2b; details in a different abstract from our group) show very similar trends with ADC decreasing at longer diffusion times due to some source of hinderance. This effect is observed perpendicular to the axons as expected (cos$^2\theta$=0), but also along the direction of the tract (cos$^2\theta$=1). Bending, fanning (Figure 1a) and undulating (Figure 1b) fibres were investigated as potential sources of the longitudinal hinderance. The results are summarized in Figure 3, where the ADC along the tract is plotted vs. diffusion time. The slightly bending 200 µm axons (orange) show very little sign of hinderance. The sharp bends of shorter simulated axons match the observed slope and shape of the curve better (in blue). The fanning pattern of the short axons shows a similar diffusion behaviour to the sharp bending geometries suggesting that fanning configurations could also underlie the data. The undulation, however, does not appear to be consistent with the data. No diffusion time dependence was observed along the axons at the scale of undulation investigated.

CONCLUSION – Diffusion along axonal tracts exhibits hinderance at long diffusion times. This effect could be used as a means to derive information about the microscopic anatomy within fibre bundles. Simulations suggest that one of the causes for restricted diffusion along fibres might be bending or fanning of axons. Simulations further indicate that gentle bending is not enough to explain diffusion data at long diffusion time, but that sharp bends are required to induce the observed relation between diffusion time and ADC. The plausibility of such configurations in the corpus callosum should be quantified in future histological investigations.

REFERENCES – [1]Mikula et al., Nat.Meth. 2012; [2]Budde & Annese, FiIN 2013; [3]Balls & Frank, MRM 2009; [4]Stiles et al., PNAS 1996.
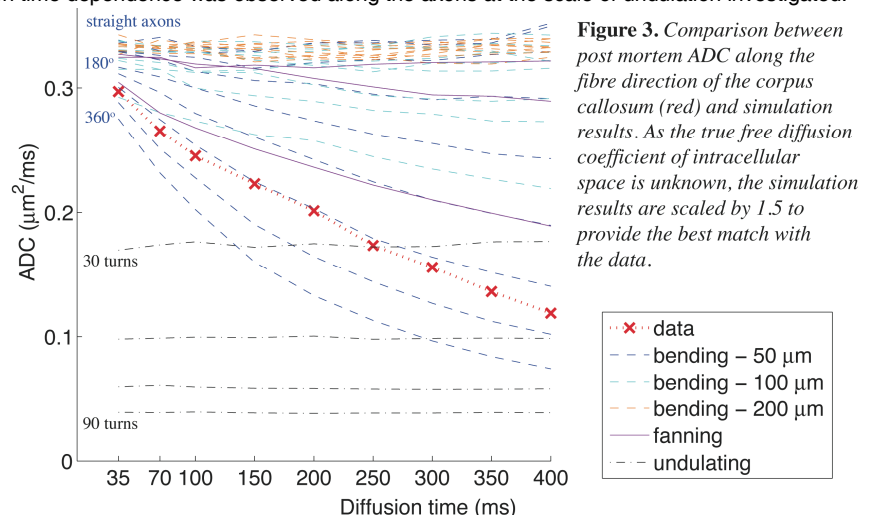
Figure 3. *Comparison between post mortem ADC along the fibre direction of the corpus callosum (red) and simulation results. As the true free diffusion coefficient of intracellular space is unknown, the simulation results are scaled by 1.5 to provide the best match with the data.*